Atmos. Meas. Tech. Discuss., 8, 7843–7878, 2015
www.atmos-meas-tech-discuss.net/8/7843/2015/
doi:10.5194/amtd-8-7843-2015

Atmospheric Measurement Techniques Discussions

Long-term variability of aerosol optical thickness in Eastern Europe over 2001–2014 according to the measurements at the Moscow MSU MO AERONET site with additional cloud and NO_2 correction

N. Y. Chubarova, A. A. Poliukhov, and I. D. Gorlova

Moscow State University, Faculty of Geography, 119991 Moscow, Russia

Received: 18 June 2015 – Accepted: 26 June 2015 – Published: 29 July 2015

Correspondence to: N. Y. Chubarova (chubarova@geogr.msu.ru)

Published by Copernicus Publications on behalf of the European Geosciences Union.

Abstract

The aerosol properties of the atmosphere were obtained within the framework of the AERONET program at the Moscow State University Meteorological Observatory (Moscow MSU MO) over 2001–2014 period. The quality data control has revealed the necessity of their additional cloud and NO_2 correction. The application of cloud correction according to hourly visual cloud observations provides a decrease in average aerosol optical thickness (AOT) at 500 nm of up to 0.03 compared with the standard dataset. We also show that the additional NO_2 correction of the AERONET data is needed in large megalopolis, like Moscow, with 12 million residents and the NO_x emission rates of about 100 kt yr^{-1}. According to the developed method we estimated monthly mean NO_2 content, which provides an additional decrease of 0.01 for AOT at 340 nm, and of about 0.015 – for AOT at 380 and 440 nm. The ratios of NO_2 optical thickness to AOT at 380 and 440 nm are about 5–6 % in summer and reach 15–20 % in winter when both factors have similar effects on UV irradiance. Seasonal cycle of AOT at 500 nm is characterized by a noticeable summer and spring maxima, and minimum in winter conditions, changing from 0.08 in December and January up to 0.3 in August. The application of the additional cloud correction removes a local AOT maximum in February, and lowered the December artificial high AOT values. The pronounced negative AOT trends of about −1–5 % yr^{-1} have been obtained for most months, which could be attributed to the negative trends in emissions (E) of different aerosol precursors of about 116 Gg yr^{-2} in E_{SO_x}, 78 Gg yr^{-2} in E_{NMVOC}, and 272 Gg yr^{-2} in E_{CO} over European territory of Russia. No influence of natural factors on temporal AOT variations has been revealed.

1 Introduction

Atmospheric aerosols are among the most important factors influencing net radiation at the top and at the bottom of the atmosphere and, therefore, affecting the whole climate

AMTD
8, 7843–7878, 2015

system (IPCC, 2013). However, still there is not enough information about their optical properties over different geographical regions. The knowledge of long-term variations of aerosol optical thickness can significantly affect the assessment of climate change, and at the same time they can be an indicator of changes in emissions of aerosol precursors (Tegen et al., 1997).

Different aerosol characteristics are possible to obtain from satellite instruments (i.e. AVHRR, MODIS, CERES, AATSR, MERIS, OMI, GLAS, SeaWiFs, MISR). However, still the ground-based measurements are characterized by the best accuracy and serve as a reference for comparisons. Ground-based aerosol networks such as GAW-PFR, AERONET, SKYNET, SibRad, and German AOD network, provide high quality aerosol measurements (http://www.wmo.int/pages/prog/arep/gaw/aerosol.html). Aerosol Robotic Network (AERONET) (http://aeronet.gsfc.nasa.gov/) has been in operation since the middle of 1990s (Holben et al., 1998) with currently more than 200 sites continuously working all over the world. AERONET is equipped by CIMEL sun/sky photometers, which provide accurate measurements of direct solar irradiance and multi-angle sky radiance from UV to near-infrared spectral region for evaluating aerosol optical thickness and many other inversion products including size distribution, effective radii, aerosol phase function, and different optical and radiative aerosol properties – refractive index, single scattering albedo, asymmetry factor, etc. (Dubovik and King, 2000).

In order to eliminate the cases, which are degraded by cloud-contamination a special cloud-screening procedure has been used in the AERONET algorithm (Smirnov et al., 2000). In addition, in the second version of the AERONET dataset (Holben et al., 2006) the correction on several optically effective trace gases (NO_2, O_3, CO_2, H_2O, CH_4) has been applied for the measurements in different channels.

The continuous aerosol measurements at the Moscow State University Meteorological Observatory (Moscow MSU MO) within the AERONET program have been in operation since August 2001. These records provide a reliable dataset for studying long-term variability of aerosol properties in the Eastern Europe, where the aerosol

AMTD
8, 7843–7878, 2015

network is rare. In addition, the auxiliary hourly cloud visual observations and measurements of different trace gases at the MSU MO over the whole period of observations enable us the data for testing the existing AERONET algorithms and improving the quality of the aerosol dataset. This is important since one can see still the effects of residual thin homogeneous cirrus cloud contamination in aerosol retrievals even in the final AERONET dataset (O'Neill et al., 2003; Uliumdjieva et al., 2005). One of the tasks of this paper is to demonstrate the effects of the additional cloud-screening procedure and NO_2 correction on evaluation of aerosol climatology in Moscow. Using the revised aerosol dataset we studied the seasonal features and long-term aerosol optical thickness (AOT) variability over the 2001–2014 period. We also tried to find explanation of the obtained AOT trends in Moscow and show the possible natural and human induced effects on its character.

2 Data description

The procedure of aerosol measurements by CIMEL AERONET sun/sky photometer and the inversion algorithms were described in numerous publications (http://aeronet.gsfc.nasa.gov/new_web/publications.html). MSU MO site utilizes the 1.2° full field CIMEL CE318 sun and sky photometer. The direct solar radiation measurements in the 340, 380, 440, 500, 675, 870, and 1020 nm channels are used for aerosol optical thickness retrievals; the measurements in the 940 nm channel are used for the evaluation of water vapor content W. In addition, direct spectral irradiance measurements are applied for the retrievals of fine and coarse aerosol modes according to the spectral deconvolution algorithm (O'Neill et al., 2001, 2003). Both sun and sky-radiance in the channels 440, 670, 870 and 1020 nm are utilized in the inversion algorithm developed by Dubovik and King (2000), which provides several important aerosol products (volume size distribution, refractive index, single scattering albedo, phase function, etc.). The uncertainty of aerosol optical thickness measurements does not exceed 0.01 in visible range and 0.02 – in UV spectral range (Eck et al., 1999). However, there are

AMTD
8, 7843–7878, 2015

some important but still not fully resolved problems, which include testing and further improvement of cloud-screening algorithm and the additional correction on NO_2 in large megalopolis like Moscow. For the improvement of these procedures, in addition, we used visual cloud observations with 1 h resolution as well and in-situ long-term measurements of NO_2 concentrations by APNA-360, Horiba Inc. (Elanski et al., 2007) at the Moscow MSU MO since 2002. The NO_2 data were used as the input parameters in the developed algorithm described in (Chubarova et al., 2010) for the independent evaluation of NO_2 content in the low troposphere over urban Moscow area. The details of the methods and the results are discussed below in the next section.

3 Results

3.1 The effects of the additional cloud-screening and NO_2 correction on aerosol climatology

3.1.1 Additional cloud-screening procedure and its effect on aerosol climatology

Since the aerosol measurements are carried out in automatic regime, a special cloud-screening procedure was developed for an automatic removal of cloud contaminating aerosol measurements (Smirnov et al., 2000). In the standard AERONET algorithm the data, which successfully pass the cloud screening procedure, are assigned to the level 1.5. After the second calibration and some additional visual checks the data are assigned to the final level 2.0. However, sometimes even the final dataset could "suffer" from the effects of thin homogeneous upper cloudiness contamination (O'Neill et al., 2003). As was mentioned in this paper "the strategy of the AERONET cloud screening was liberal; to interfere as little as possible with coarse mode events such as dust incursions and thus to accept the inevitability of some thin homogeneous cloud data,

AMTD
8, 7843–7878, 2015

being admitted into the database." Hence, the question remains, how important can be this effect. Will it significantly affect the aerosol climatology?

The influence of the cloud contamination on aerosol properties was also discussed in Uliumdzhieva et al. (2005). In this paper the application of the standard cloud visual observations as an additional cloud-screening filter was proposed. We showed there that the existing standard cloud-screening algorithm works perfectly, when aerosol measurements are contaminated by low layer convective cloudiness. However, thin homogenous cirrus clouds could significantly influence the aerosol retrievals. Balancing between the substantial decrease in case number and the accuracy of the retrievals of aerosol properties we showed that the best results were obtained when total cloudiness $N_{\text{total}} > 9$ was used as a filter threshold during March–October period, when 100 % cloud contaminated data were removed in overcast cloud conditions. For November–February conditions the filter threshold is more strict ($N_{\text{total}} > 6$) since solar elevation in Moscow is low ($h_{\text{noon}} < 25^{\circ}$) at this time and a well-known effect of significant visual cloud amount increase towards the horizon plays a vital role.

Using this approach we obtained a revised dataset with additional visual cloud-screening over the whole 2001–2014 period of observations in Moscow. Figure 1a and b shows the absolute and relative differences between the standard monthly mean aerosol optical thickness at 500 nm (AOT500) and additionally cloud-screened AOT500 values, as well as the differences in water vapor content, Angstrom exponent, and variation in day number over the whole period of measurements. One can see a substantial systematically overestimation of monthly mean aerosol optical thickness at 500 nm in the standard AERONET dataset up to 0.03 for several months. For all months (except September and November) the error is higher than 0.01, which corresponds to the uncertainty of AOT measurements ($\varepsilon = 0.01$, depicted by the line in Fig. 1). In some years the difference can even exceed 0.1 (for example, in February 2005 and October 2012). Due to existing AOT seasonal change the relative difference in AOT500 has a noticeable minimum in summer (5 %) and the increase up to 20–30 % during winter months when the occurrence of upper cloudiness is high and AOT is low. There

AMTD
8, 7843–7878, 2015

is also discernible underestimation of Angstrom exponent in the standard AERONET dataset due to the influence of close to neutral scattering on large cirrus particles, which contaminate AOT values which are used for the Angstrom exponent evaluation. The relative bias in Angstrom exponent has also some tendency towards higher underestimation (from −1–2 to −6 %) in the standard product in cold period. Both positive AOT difference and negative Angstrom exponent difference clearly indicate the reliable elimination of cloud contaminated cases after the application of additional cloud filter. It is interesting that water vapor content W is also overestimated in cloud contaminated conditions up to 0.05–0.07 cm (or 15–20 %) during winter months possibly due to the additional absorption by ice and water particles.

After the application of an additional cloud filter the day number significantly decreases (see Fig. 1b): up to 7–20 % during warm period, and 25–45 % in cold period due to higher occurrence of overcast upper layer cloudiness and the application of stricter filter. Note, that small day number with aerosol observations in winter due to cloudy conditions results in large relative changes of the removed day number even when only 1–2 days are removed from the initial statistics.

3.1.2 NO_2 correction algorithm and the effects of the revised NO_2, climatology on AOT estimations

The version 2 AERONET algorithm includes the correction on different trace gases content (http://aeronet.gsfc.nasa.gov/new_web/Documents/spectral_corrections_v2.pdf). Among them nitrogen dioxide (NO_2) has a significant absorption in UV and visible channels, especially over the urban/industrial areas.

We should emphasize that Moscow is a large megalopolis with significant level of NO_x emission of about 100 kt yr^{-1} (Ivanov et al., 2012). According to the data of Mosecomonitoring Agency the actual NO_2 surface concentrations in clean background conditions near Moscow are about 70 % lower than those observed in Moscow (Report on the State of the Environment in Moscow, 2014). The spectral correction of aerosol optical thickness on NO_2 in the AERONET algorithm is made according to the SCIA-

AMTD
8, 7843–7878, 2015

MACHY climatology data over the 2003–2005 period (http://www.temis.nl/airpollution/no2.html) (Eskes et al.,2004). However, other studies have revealed much higher NO_2 content over Moscow (Ivanov et al., 2012). According to satellite data the NO_2 tropospheric content over megacities reach high level (Hiboll et al., 2013). Our aerosol comparisons in urban and background conditions (Chubarova et al., 2011) also demonstrated the existence of the residual NO_2 contamination over Moscow, which can be seen in a specific character of AOT spectral difference between the parallel measurements in Moscow and in Zvenigorod background conditions (see Fig. 3 and the discussion in Chubarova et al., 2011). This residual NO_2 contamination is caused by much higher NO_2 content in Moscow than that accounted in the AERONET algorithm.

In order to exclude the effects of NO_2 underestimation in AOT retrievals over urban Moscow area we applied the algorithm for evaluating the NO_2 content, which has been developed recently (Chubarova et al., 2009, 2010). For accounting the NO_2 amount up to the height of 350 m we utilized the developed parameterizations of its content within 350 m according to in-situ long-term NO_2, measurements in the boundary layer from ground to 350 m in several points of Moscow (at the Ostankino tower and at the top of Moscow State University Building). These data were combined with the results of photochemical model, which had been adapted to the available experimental data on different chemical constituents and meteorological conditions in the boundary layer. As a result, different weighting coefficients for summer and winter conditions were obtained for different layers: 0–350 m, 350–1000 m, and 1000–2000 m. Note, that tropospheric and especially boundary layer NO_2 content in urban areas has the most important contribution to the total NO_2 content and is several times higher than that in background conditions (Richter et al., 2005; Hiboll et al., 2013). Therefore for the altitudes higher 2 km we applied the climatological NO_2 values according to numerous data of aircraft measurements (Bruns et al., 2006; Heland et al., 2002; Martin et al., 2006). They are about 0.01 ppb for the altitudes of 2–5 km, and are characterized by linear decrease to approximately 0.01 ppb at 12 km. In the stratosphere the NO_2 profile corresponds to the data published in (Bruns, 2004) according to the direct measurements in Europe

AMTD
8, 7843–7878, 2015

and Northern America. Totally the NO_2 content at the altitudes higher 2 km is relatively small comprising about 0.24 DU. (0.6×10^{16} mol cm^{-2}).

Figure 2a and Table 1 show the resulting monthly mean NO_2 content obtained according to the proposed method. One can see that the maximum NO_2 content is observed in February and elevated NO_2 values are recorded in December–March period due to higher emissions from power stations during the heating season and larger NO_2 life time in winter conditions. Figure 2a also demonstrates seasonal variations of NO_2 content, which is used in the standard AERONET algorithm. One can see that the new NO_2 climatology is 2–3 times higher than the standard AERONET NO_2 climatology, which is applied in the AERONET aerosol correction algorithm. Since these NO_2 amounts were obtained for the 2003–2005 period, we also compared them with the NO_2 retrievals over the same period according to the proposed method. As it is seen in Fig. 2a, no any statistically significant difference between the revised NO_2 content climatology is detected between the 2002–2013 and 2003–2005 periods.

The values obtained from the new NO_2 climatology are well coincided with the results of direct NO_2 retrievals using MAX-DOAS algorithm (Ivanov et al., 2012) over the same site. On average, their NO_2 estimates, in the boundary layer in Moscow are about 1.1 DU (0.5–1.8DU) while our assessments after excluding the stratospheric NO_2 content give the close value of about 1.2 DU.

The estimated NO_2 optical thickness (OT_{NO_2}) in different CIMEL spectral channels is shown in Fig. 2b. The most pronounced effects of OT_{NO_2} = 0.02–0.03 are observed for 380 and 440 nm channels due to the strongest NO_2 absorption there. At the same time, NO_2 optical thickness obtained from the standard AERONET algorithm is much smaller and does not exceed OT_{NO_2} = 0.013 at 380 nm in March. New NO_2 climatology provides NO_2 optical thickness, which is 2–4 times higher than the values in the standard AERONET dataset for Moscow urban conditions. It should be emphasized that the added OT_{NO_2} values are close to the uncertainty threshold of aerosol optical thickness evaluation of $\sim$ 0.02 at 340 nm and are usually higher than the uncertainty threshold for AOT at other wavelengths especially, in winter and spring conditions, which should

AMTD
8, 7843–7878, 2015

be necessary to take into account. The obtained monthly mean NO_2 content can be considered as a typical level for large megalopolis with 12 million residents and the NO_x emission rates of about 100 kt yr^{-1}.

Since the uncertainty in AOT according to the additional correction on the revised NO_2 optical thickness has a spectral character the effect is also expressed in the retrievals of the Angstrom exponent (α). One can see in Table 1 a decrease (in absolute values) in the $\alpha_{440-870}$ retrievals of about 0.06–0.3 for different months mainly due to the reduction of AOT at 440 nm after applying the higher values of OT_{NO_2} from the new NO_2 climatology. On the contrary, the revised Angstrom exponent retrievals in UV spectral region increase up to 0.15–0.6 after additional NO_2 correction. Both procedures lead to decreasing in the second derivative and may affect the inverse RT solution in the AERONET algorithm (Dubovik and King, 2000), especially in case, when OT_{NO_2} values are close to aerosol optical thickness.

Seasonal variations of OT_{NO_2} to AOT ratios at different wavelengths are shown in Fig. 2c. One can see that the maximum effect is observed for the ratio at 380 and 440 nm, comprising about 15–20 % in winter and 5–6 % in other seasons. This ratio is smaller at 340 and 500 nm varying from 10 % in winter to 2–3 % in other seasons. Hence, the most substantial changes in aerosol properties and, hence, solar irradiance due to NO_2 correction are observed during cold period. This implies the increase in the effects of NO_2 absorption during winter time.

We estimated relative attenuation due to monthly mean NO_2 and aerosol optical thickness for erythemal and longwave UV 300–380 nm irradiance at ground according using the TUV model (Madronich and Flocke, 1998) with 8-stream DISORT solver and pseudo spherical corrections. Similar effects of NO_2 and AOT of about 4–7 % are observed during winter time, while in summer the effects of AOT reach 14 % compared with 1–2 % due to NO_2 (Fig. 2d). There is a pronounced amplification of NO_2, effects for longwave UV 300–380 nm irradiance due to the increase of the effective wavelength (from ~ 305–315 nm for erythemal radiation to ~ 345 nm – for UV irradiance 300–380 nm), where the NO_2 absorption coefficients are much higher. In addi-

AMTD
8, 7843–7878, 2015

tion, using the on-line calculator (http://litms.molnet.ru/csif/index.php) developed in the Institute of Moleculer Physics of RRC "Kurchatov Institute" we estimated the effects of NO_2 on total shortwave irradiance, which are about 0.5 % in summer and 2.5 % in winter depending on NO_2 content and solar zenith angle.

As a result, we have applied the NO_2 correction to monthly mean AOT values for the whole AERONET dataset in Moscow since 2001. We should note, that large NO_2 content can be also observed in forest fire smoke plumes, however, due to large aerosol amount and small OT_{NO_2}/AOT ratios its radiative effect should be small compared with the aerosol radiative impact.

NO_2 effects on other aerosol characteristics are also existing, however, we do not consider them in this study. According to several case studies we showed the effects of NO_2 on the retrievals of single scattering albedo, which can increase up to 0.02 when the ratio OT_{NO_2}/AOT at 440 nm is about 10 % (Chubarova and Dubovik, 2004). The influence of NO_2 on the retrievals of aerosol size distribution is also pronounced with the artificial bias towards smaller particles overestimating the fine mode fraction of about $dV/d\ln r = 0.02\,\mu m^3\,\mu m^{-2}$ at $r = 0.05$–$0.065\,\mu m$ and decrease over 0.01–$0.03\,\mu m^3\,mm^{-2}$ at 0.11–0.15 µm for typical air pollution conditions. However, in overall the fine mode fraction due to accounting for NO_2 content changes only on 1–5 % (Chubarova and Dubovik, 2004).

A full scheme of aerosol correction for Moscow MSU MO aerosol measurements is shown in Fig. 3. The final aerosol product is attributed to so-called level 2.5 just to be in the mainstream of the AERONET standard level ranks. Currently, the correction has been fulfilled only for the aerosol parameters retrieved from direct solar measurements (aerosol optical thickness and Angstrom exponent). The standard and the revised monthly mean spectral AOT dependence over the 2001–2014 period after the cloud and NO_2, corrections is shown in Fig. 4. The revised spectral dependencies are characterized by more smooth spectral character due to the influence of spectral NO_2 correction. The total difference in annual mean AOT values due to additional ac-

AMTD
8, 7843–7878, 2015

count for cloud and NO_2 corrections is about 0.04 in UV, 0.02 in visible, and 0.01 in near-infrared spectral ranges.

3.2 Seasonal changes in aerosol optical thickness in Moscow according to the revised dataset

After additional cloud and NO_2 correction we obtained a revised dataset of aerosol optical thickness, water vapor content and Angstrom exponent over the 2001–2014 period. Figure 5 shows the seasonal changes of monthly mean AOT500, AOT380, and Angstrom exponent $\alpha_{440-870}$ from the revised dataset, the dataset with only additional cloud correction, and from the standard AERONET level 2.0 dataset. The difference between the cloud-corrected and the revised aerosol optical thickness demonstrates the effect of NO_2 additional correction. The revised AOT seasonal cycle is characterized by a pronounced summer maximum reaching AOT500 = 0.3 in August, an additional maximum in April (AOT500 = 0.22), and minimum in December and January (AOT500 = 0.08). One can see that the application of the additional cloud correction removes a local AOT maximum in February, and lowered the December artificial high AOT values. The application of the new NO_2 climatology provides the decrease in AOT all over the year and does not significantly change the AOT seasonal cycle. The maximum effects of NO_2 can be seen in correction of AOT at 380 nm due to the highest NO_2 absorption coefficients. The effects of additional NO_2 and cloud correction are comparable for AOT380 and AOT440, while for AOT at other wavelengths the additional cloud correction plays more vital role. The main statistics of revised AOT, water vapor content and Angstrom exponent are presented in Table 2.

In Moscow Angstrom exponent has a pronounced maximum in summer months, which had been also documented for European conditions (Hsu et al., 2014; Chubarova, 2009). The revised $\alpha_{440-870}$ values are characterized by much more noticeable seasonal dependence with a substantial decrease in December.

Figure 6 presents three-dimensional distributions of monthly mean, 50 % quantile, maximum and minimum AOT500 values over the 2001–2014 period. The AOT maxi-

AMTD
8, 7843–7878, 2015

mum in spring (and, especially, in April) is typical for almost all years and is a characteristic feature for the whole Eastern European plane. It can be explained by the circulation pattern from South–East of Russia and Kazakhstan with dust advection from semi-deserts and steppes, as well as by the accumulation of the dust after snow melting, and the beginning of agricultural season with the prescribed fires. At the same time, relatively small precipitation prevents wet deposition of aerosol particles and contributes to their accumulation. In April, for example, the precipitation is only 41 mm, which is about 30 % smaller than the annual monthly mean value (Chubarova et al., 2014). The local June minimum is observed due to the increase in precipitation, dominating the northern air advection from Scandinavian regions, more intensive uptake of aerosol by grass and leaves, and comparatively high water store in soil and vegetation, which can also prevent active mineral dust aerosol formation. According to monthly mean data summer AOT500 maximum is observed in August. However, AOT500 50 % quantile has the maximum in July, when the high temperature provides favorable conditions for the second aerosol generation and accumulation of aerosol (see also Fig. 5 and Table 2). The bias towards the fall in monthly mean AOT500 is observed due to the episodes with forest and peat bog fires with high aerosol loading in 2002 (July, August and September) and 2010 (July, August) (Chubarova et al., 2012).

In winter, there is a minimum in AOT due to wet deposition of aerosol during active cyclonic processes and the absence of favorable conditions for second aerosol generation. Note, that low AOT in December and February are observed only after NO_2, and cloud correction.

The described AOT seasonal changes occur almost every year, except 2006 (see Fig. 6). AOT daily maxima are also observed every year in spring and in summer. During the intensive forest fires in Moscow regions in 2002 and 2010 the daily maximum AOT500 has reached 2.3 in July 2002 and 3.7 in August 2010. However, there are no any seasonal changes in daily minima – the AOT500 varies within 0.02–0.05 throughout the year. Even during the long-term forest fires episodes very low and extremely high AOT values are observed during the same month. This phenomenon takes place

AMTD
8, 7843–7878, 2015

due to changes in wind direction and advection of fresh as well as due to effective wet deposition of aerosol particles from the atmosphere which, for example, was observed in August 2010.

3.3 Long-term AOT trends in Moscow and their possible reasons

The continuous aerosol measurements since 2001 provide a perfect tool for studying long-term variability of aerosol properties over 14 years. Table 3 summarizes the correlation coefficients and AOT relative temporal changes for different months, except January and December, when the statistics is too low due to prevailing cloudy conditions. One can see a decrease in monthly mean AOT500 with the rate of about ~ 1–$5\,\%\,\mathrm{yr}^{-1}$ for most months, except June and November. However, the statistically significant trends of mean and daily maxima AOT500 values at $P = 95\,\%$ are observed only in April, May and September. After excluding the intensive fire periods in 2002 and 2010 the significance of AOT trend remains the same, but its values have changed, for example, from 10 to $3\,\%\,\mathrm{yr}^{-1}$ in September. In April and September statistically significant negative trends were also obtained for 50 % quantile AOT500. So we can state that the most significant AOT decrease is observed in spring and fall periods.

Relative changes in annual mean and 50 % quantile values of aerosol optical thickness at different wavelengths in UV, visible and near-infrared spectral range are shown in Fig. 7. Negative annual AOT trends are about -2.3 and $-1.7\,\%\,\mathrm{yr}^{-1}$ at 500 nm, -2.7 and $-2.9\,\%\,\mathrm{yr}^{-1}$ at 340 nm, and -1.8 and $-1.1\,\%\,\mathrm{yr}^{-1}$ at 1020 nm respectively for the mean and 50 % quantile values. For the annual mean AOT the negative trend is statistically significant at $P = 95\,\%$ over the whole spectral range and is characterized by a 15–20 % drop over the last four years, while for annual 50 % quantile AOT values the significant trend is observed only at 340 and at 500 nm. There is no statistically significant trend in the annual 50 % quantile AOT at 1020 nm that could mean preserving the same coarse mode particles content in typical conditions. This could be also confirmed by the decrease in monthly mean Angstrom exponent obtained within a spectral range of 440–870 nm during summer period. We should emphasize that the trend obtained

AMTD
8, 7843–7878, 2015

for annual mean AOT values is much more sensitive to the fire smoke episodes with extremely high aerosol loading (for example, forest fires in 2002 and 2010). Annual 50 % quantile AOT values are not sensitive to such outbursts, therefore their interannual changes better describe the temporal changes of typical aerosol.

The negative AOT trends in 21 century are observed over many regions in Europe. For example, according to satellite dataset Yoon et al. (2014) has revealed a distinct AOT decrease over western Europe of about −40 % from 2003 to 2008. The same negative trends over 1997 to 2010 in Europe was obtained in (Hsu et al., 2012) according to SeaWiFS measurements. In Putaud et al. (2014) the negative trends in AOT and some other aerosol characteristics were also obtained in Northern Italy over the 2004–2010 period.

There can be several natural or anthropogenic reasons for these negative AOT trends. In order to study the effect of anthropogenic emissions we used the officially reported emission data from the Centre on Emission Inventories and Projections WebDab – EMEP database (http://www.ceip.at/webdab_emepdatabase/). Figure 8a presents temporal variations in emissions of different main aerosol precursors over the European part of Russia, which can affect the secondary aerosol generation in Moscow. One can see a statistically significant at $P = 95$ % decrease in SO_x emission of about 116 $Gg\,yr^{-2}$, the negative trend in emission of Non-methane volatile organic compound (NMVOC) of about 78 $Gg\,yr^{-2}$, as well as in CO emission (272 $Gg\,yr^{-2}$). There is also a substantial decrease in NO_x, over European part of Russia during the last years, however, the data for 2012–2014 period are unavailable yet. No trend is observed in concentration of particulate matter with the diameter less 2.5 µm ($PM_{2.5}$). The comparison of temporal variability of main aerosol precursors over the European part of Russia and in Moscow is shown in Fig. 8b. There we also present the trend in annual 50 % quantile AOT500, which is not sensitive to the extremely high aerosol loading during the Moscow 2002 and 2010 fire episodes. One can see the absence of local changes in SO_x in Moscow compared with a distinct negative trend in SO_x up to −7 % a year over the whole territory of European part of Russia, which can be observed

AMTD
8, 7843–7878, 2015

due to change in fuel from coal to gas. In Moscow this change of fuel has been made at the end of 1980s. Note also, that the high median AOT values in 2006 correspond well with the elevated emission of SO_x both in Moscow and at the whole European plain as well as the emission of NO_x – in Moscow. The last years are characterized by a decrease in NO_x emission both in Moscow and at the European part of Russia possibly due to improving the quality of petrol standards. However, according to (Hiboll et al., 2013) the negative trend in NO_2 ($\sim -1.6\,\%\,yr^{-1}$) is not significant in Moscow. As a result, we assume that negative trend in AOT could be observed due to decrease in anthropogenic emissions of SO_x, NMVOC and CO over European plain, which play a significant role in second aerosol generation especially during warm period.

However, natural AOT variations can be also taken into account. For example, since AOT is characterized by a significant decrease from south-east to the north in Europe (Chubarova, 2009) natural AOT interannual variability can be observed due to the year-to-year variability of different air mass advection. Wet aerosol deposition, regulated by precipitation, can also play an important role in year-to-year AOT variability. In addition, the enhancement of the dynamic stability of the atmosphere can be also an effective factor leading to the stagnation of air and, hence, to the aerosol accumulation. As a parameter characterizing the atmospheric instability we used the convective available potential energy (CAPE) (Barry and Chorley, 1998). The CAPE data from the ERA-Interim re-analysis over Moscow (36–38° E, 55–56° N) were taken for the days, when the aerosol measurements were made.

As a result, multiple regression analysis has been applied for studying the relationship of monthly mean AOT500 with temperature (as an indicator of air advection), precipitation, wind speed, wind direction and CAPE characteristics according to the Moscow dataset over the whole period of measurements. However, the analysis revealed the absence of significant AOT correlation with any of the characteristics considered. This means that natural factors might not be responsible for the negative AOT trend in the Moscow area.

AMTD
8, 7843–7878, 2015

4 Discussion

We propose the additional cloud screening correction and the revised NO_2 data for large megacity conditions for obtaining the highest quality dataset of aerosol properties. Small but systematical AOT500 overestimation up to 0.03 in the standard AERONET dataset was received due to the effects of uniform cirrus clouds. This overestimation is usually higher than the uncertainty of AOT measurements. In some years the application of additional cloud filter resulted in the AOT bias of more than 0.1. The contribution of this difference for AOT500 has minimum in summer (5 %) and increase up to 20–30 % for winter months when the occurrence of upper cloudiness is high, and AOT values are low. Since the effects of additional cloud-screening are distinct, its application could be helpful at other AERONET sites. The information on the visual cloud observations can be taken from meteorological stations for the cases when it is necessary to obtain the best aerosol quality statistics over the historical periods of aerosol measurements. According to our analysis, about 80 % of AERONET sites are located within 60 km from the nearest meteorological station. This is enough for removing the cloud-contaminated aerosol measurements, since upper layer cirrus cloudiness occupies extremely large spatial fields of thousands of kilometers (Radiation in cloudy atmosphere, 1984). It is also possible to verify the current aerosol datasets using the cloud data from the automatic total sky imagers, which have been already in operation at several sites (O'Neill et al., 2003).

For additional NO_2 correction a new NO_2 content climatology over Moscow has been applied according to the algorithm, which has been developed recently (Chubarova et al., 2010) on the base of in-situ NO_2 concentration measurements at different altitudes and the results of photochemical model. The new monthly mean NO_2 content is two-three times higher, than that in the AERONET dataset, which is used for aerosol correction due to extremely large NO_x emission in large megacity, like Moscow. The most pronounced effects of OT_{NO_2} = 0.02–0.03 are observed at 380 and 440 nm channels due to the strongest NO_2 absorption. The obtained monthly mean NO_2 values can

AMTD
8, 7843–7878, 2015

be considered as typical values for megalopolis conditions with 12 million residents and the NO_x emission rates of about 100 kt yr^{-1} (Ivanov et al., 2012). The NO_2 correction over other megacities can be also made according to long-term satellite NO_2 retrievals but after their rigorous validation.

Seasonal variations of OT_{NO_2} to AOT ratio at 380 and 440 nm vary from 15–20 % in winter to 5–6 % in warm period. This ratio is much smaller at 340 and 500 nm changing from 10 % in winter to 2–3 % in warm period. Hence, the most substantial changes in aerosol properties and, hence, solar irradiance due to NO_2 correction would be observed during cold period. According to radiative modeling this results in similar effects of NO_2 and aerosol in winter in UV spectral region, which is about 4–7 %. For shortwave irradiance the NO_2 effect in Moscow changes within 0.5–2.5 % and also increases in winter.

The total difference in annual mean AOT values due to the additional account for cloud and NO_2 corrections is about 0.04 in UV, 0.02 in visible, and 0.01 in near-infrared spectral range. The revised aerosol product after the application of additional cloud and NO_2 correction is attributed to so-called level 2.5 to be in the mainstream of the AERONET standard level ranks. Currently, the correction has been fulfilled only for the aerosol parameters retrieved from direct solar measurements (aerosol optical thickness, Angstrom exponent, and water vapor content).

The revised dataset of monthly mean aerosol optical thickness and Angstrom exponent in Moscow was used for studying seasonal changes as well as AOT long-term variability over the 2001–2014 period.

The corrected AOT mean seasonal cycle is characterized by a pronounced summer maximum, an additional spring maximum, and minimum in winter conditions (December–January). The application of the additional cloud correction removes a local AOT maximum in February, and lowered the December artificial high AOT values. After the application of additional filters we also obtained much more noticeable seasonal dependence of Angstrom exponent with the maximum during summer period.

AMTD
8, 7843–7878, 2015

There are pronounced statistically significant negative trends at $P = 95\,\%$ in temporal variation of mean and 50 % quantile AOT500 values for some months over 2001–2014. We also found a decrease in monthly mean AOT500 changes of about -1–$5\,\%\,yr^{-1}$ for most months, however, the statistically significant trends of mean and daily maxima AOT500 values are observed in April, May and September. The most significant temporal changes in AOT are observed in spring and fall period. This is especially important, since April is characterized by local seasonal AOT maximum. Removal of AOT observed during the intensive fire periods in 2002 and 2010 does not change the significance of the results, but modify the value of AOT500 relative change.

There is also a statistically significant negative trend at $P = 95\,\%$ in annual mean AOT variations over the whole spectral range with a pronounced 15–20 % drop during the last four years. At the same time considering annual 50 % quantile AOT variation we found a statistically significant trend in AOT only at 340 and 500 nm. No similar tendency in AOT at 1020 nm was obtained, that could mean no temporal changes in coarse mode particles during the whole period of observations in *typical* conditions, which are better described by the analysis of 50 % quantile AOT.

To understand the cause of the negative trends we used the data from the Centre on Emission Inventories and Projections (WebDab – EMEP database). According to these data we showed that the decrease in AOT can be observed in 21 century due to statistically significant at $P = 95\,\%$ negative trends in SO_x emission of about $116\,Gg\,yr^{-2}$, in NMVOC emission of about $78\,Gg\,yr^{-2}$, and in CO emission ($272\,Gg\,yr^{-2}$). We found that the high median AOT values in 2006 correspond well with the elevated emission of SO_x both in Moscow and at the whole European plain, as well as with NO_x – in Moscow. The last four years are characterized by some decrease in NO_x, emission both in Moscow and at the European part of Russia possibly due to improving the quality of petrol standard. However, the NO_2 trend in Moscow is not statistically significant. We also studied the possible effect of natural factors in AOT variability. No statistically significant correlation was obtained in AOT relationship with different meteorological parameters and CAPE. This means the importance of the anthropogenic

AMTD
8, 7843–7878, 2015

factor (negative emissions of aerosol precursors) for attributing the negative AOT trend in Moscow.

5 Conclusions

We show the necessity of additional cloud and NO_2 correction for retrieving the best quality aerosol climatology. The application of the additional cloud-screening filters revealed a noticeable positive bias of up to 0.03 in monthly mean aerosol optical thickness compared with the results obtained from the standard algorithm.

A new NO_2 climatology over Moscow has been obtained. Its application demonstrates that tropospheric NO_2 content in Moscow is two-three times larger than that applied in the standard AERONET algorithm. The additional NO_2 correction of aerosol optical thickness is about 0.01 at 340 nm, and 0.015 – at 380 and 440 nm.

The total difference in annual mean AOT values due to the additional account for cloud and NO_2 correction is about 0.04 in UV, 0.02 in visible, and 0.01 in near-infrared spectral range, which are higher than the uncertainty of AOT measurements.

The revised dataset was used for the analysis of seasonal and year-to-year variability of aerosol optical thickness in Moscow over the 2001–2014 period. We have revealed the distinct seasonal cycle in AOT500 values changing from 0.08 in December up to 0.3 in August as well as summer maximum in Anstrom exponent.

The interannual changes in aerosol properties reveal distinct negative trends, which are statistically significant in April, May and September. We show that the main reason for the AOT decrease could be negative trends in emissions of different aerosol precursors over European Plain according to the WebDab – EMEP database. We showed that the AOT negative trend can be observed due to a noticeable decrease in SO_x, NMVOC and CO emissions at the European Plain. The analysis of variability in natural factors has not revealed their influence on negative AOT trends. However, further studies will be helpful for understanding the role of specific emissions and their interaction with changing weather conditions.

AMTD
8, 7843–7878, 2015

Acknowledgements. We would like to thank A. Smirnov (NASA Goddard Space Flight Center) for fruitful discussions. The work was partially supported by RFBR grants #13-05-00956 and #15-05-03612.

References

Barry, R. G. and Chorley, R. J.: Atmosphere, Weather and Climate, 7th edn., Routledge, Taylor & Francis Group, USA, 80–81, 1998.

Bruns, M.: NO_2 retrieval using airborne multiaxis differential optical absorption spectrometer (AMAXDOAS) data, Dissertation, Universitat Bremen, Germany, 174 pp., 2004.

Bruns, M., Buehler, S. A., Burrows, J. P., Richter, A., Rozanov, A., Wang, P., Heue, K. P., Platt, U., Pundt, I., and Wagner, T.: NO_2 profile retrieval using airborne multi axis UV-visible skylight absorption measurements over central Europe, Atmos. Chem. Phys., 6, 3049–3058, doi:10.5194/acp-6-3049-2006, 2006.

Chubarova, N. and Dubovik, O.: The sensitivity of aerosol properties retrievals from AERONET measurements to NO_2 concentration over industrial region on the example of Moscow, Optica Pura y Aplicada, A. Hidalgo (Spain), 37, 3315–3319, 2004.

Chubarova, N., Nezval', Ye., Sviridenkov, I., Smirnov, A., and Slutsker, I.: Smoke aerosol and its radiative effects during extreme fire event over Central Russia in summer 2010, Atmos. Meas. Tech., 5, 557–568, doi:10.5194/amt-5-557-2012, 2012.

Chubarova, N. E., Larin, I. K., and Lezina, E. A.: Experimental studies and modeling of nitrogen dioxide variations in the lowest troposphere layer in Moscow, Newsletter Moscow State University, series 5, Geography, 5, 11–18, 2010.

Chubarova, N. E., Nezval', E. I., Belikov, I. B., Gorbarenko, E. V., Eremina, I. D., Zhdanova, E. Yu., Korneva, I. A., Konstantinov, P. I., Lokoshchenko, M. A., Skorokhod, A. I., and Shilovtseva, O. A.: Climatic and environmental characteristics of Moscow megalopolis according to the data of the Moscow State University Meteorological Observatory over 60 years Russian Meteorology and Hydrology, Allerton Press Inc., USA, 39, 9, 602–613, 2014.

Chubarova, N. Y.: Seasonal distribution of aerosol properties over Europe and their impact on UV irradiance, Atmos. Meas. Tech., 2, 593–608, doi:10.5194/amt-2-593-2009, 2009.

Chubarova, N. Y., Larin, I. K., Lebedev, V. V., Partola, V., Lezina, E. A., and Rublev, A. N.: Experimental and model study of changes in spectral solar irradiance in the atmosphere of

AMTD
8, 7843–7878, 2015

large city due to tropospheric NO_2 content, current problems in atmospheric radiation, in: Proceedings of the International Radiation Symposium (IRC/IAMAS), AIP Conference Proceedings, 3–8 August 2008, Foz do Iguacu, Brasil, 1100, 459–462, doi:10.1063/1.3117019, 2009.

Chubarova, N. Y., Sviridenkov, M. A., Smirnov, A., and Holben, B. N.: Assessments of urban aerosol pollution in Moscow and its radiative effects, Atmos. Meas. Tech., 4, 367–378, doi:10.5194/amt-4-367-2011, 2011.

Collaud Coen, M., Andrews, E., Asmi, A., Baltensperger, U., Bukowiecki, N., Day, D., Fiebig, M., Fjaeraa, A. M., Flentje, H., Hyvärinen, A., Jefferson, A., Jennings, S. G., Kouvarakis, G., Lihavainen, H., Lund Myhre, C., Malm, W. C., Mihapopoulos, N., Molenar, J. V., O'Dowd, C., Ogren, J. A., Schichtel, B. A., Sheridan, P., Virkkula, A., Weingartner, E., Weller, R., and Laj, P.: Aerosol decadal trends – Part 1: In-situ optical measurements at GAW and IMPROVE stations, Atmos. Chem. Phys., 13, 869–894, doi:10.5194/acp-13-869-2013, 2013.

Dubovik, O. and King, M. D.: A flexible inversion algorithm for retrieval of aerosol optical properties from Sun and sky radiance measurements, J. Geophys. Res., 105, 20673–20696, 2000.

Eck, T. F., Holben, B. N., Reid, J. S., Dubovik, O., Smirnov, A., O'Neill, N. T., Slutsker, I., and Kinne, S.: Wavelength dependence of the optical depth of biomass burning, urban and desert dust aerosols, J. Geophys. Res., 104, 31333–31349, 1999.

Elansky, N. F., Lokoshchenko, M. A., Belikov, I. B., Skorokhod, A. I., and Shumskii, R. A.: Variability of trace gases in the atmospheric surface layer from observations in the city of Moscow, Izvestiya, Atmospheric and Oceanic Physics, 43, 219–231, 2007.

Eskes, H. J. and Boersma, K. F.: Averaging kernels for DOAS total-column satellite retrievals, Atmos. Chem. Phys., 3, 1285–1291, doi:10.5194/acp-3-1285-2003, 2003.

Feigelson, E.: Radiation in a Cloudy Atmosphere, Reidel Publishing Company, Dordrecht, the Netherlands, 1984.

Heland, J., Schlager, H., Richter,. A. and Burrows, J. P.: First comparison of tropospheric NO_2 column densities retrieved from GOME measurements and in situ aircraft profile measurements, Geophys. Res. Lett., 29, 20, 1983, doi:1029/2002GL015528, 2002.

Hilboll, A., Richter, A., and Burrows, J. P.: Long-term changes of tropospheric NO_2 over megacities derived from multiple satellite instruments, Atmos. Chem. Phys., 13, 4145–4169, doi:10.5194/acp-13-4145-2013, 2013.

AMTD
8, 7843–7878, 2015

Holben, B. N., Eck, T. F., Slutsker, I., Tanre, D., Buis, J. P., Setzer, A., Vermote, E., Reagan, J. A., Kaufman, Y. J., Nakajima, T., Lavenu, F., Jankowiak, I., and Smirnov, A.: AERONET – a federated instrument network and data archive for aerosol characterization, Remote Sens. Environ., 66, 1–16, 1998.

Holben, B. N., Eck, T., Slutsker, I., Smirnov, A., Sinyuk, A., Schafer, J., Giles, D., and Dubovik, O.: AERONET Version 2.0 quality assurance criteria, in: Remote Sensing of the Atmosphere and Clouds, edited by: Tsay, S.-C., Nakajima, T., Singh, R. P., and Sridharan, R., in: Proc. of SPIE, Goa, India, 13–17 November, 6408, 2006.

Hsu, N. C., Gautam, R., Sayer, A. M., Bettenhausen, C., Li, C., Jeong, M. J., Tsay, S.-C., and Holben, B. N.: Global and regional trends of aerosol optical depth over land and ocean using SeaWiFS measurements from 1997 to 2010, Atmos. Chem. Phys., 12, 8037–8053, doi:10.5194/acp-12-8037-2012, 2012.

IPCC: Climate Change 2013: The Physical Science Basis, Contribution of Working Group I to the Fifth Assessment Report of the Intergovernmental Panel on Climate Change, Cambridge University Press, Cambridge, United Kingdom and New York, NY, USA, 1535 pp., 2013.

Ivanov, V. A., Elokhov, A. S., and Postylyakov, O. V.: On the possibility of estimating the volume of NO_2 emissions in cities using zenith spectral observations of diffuse solar radiation near 450 nm, Atmospheric and Oceanic Optics, 25, 434–439. 2012.

Kanaya, Y., Irie, H., Takashima, H., Iwabuchi, H., Akimoto, H., Sudo, K., Gu, M., Chong, J., Kim, Y. J., Lee, H., Li, A., Si, F., Xu, J., Xie, P.-H., Liu, W.-Q., Dzhola, A., Postylyakov, O., Ivanov, V., Grechko, E., Terpugova, S., and Panchenko, M.: Long-term MAX-DOAS network observations of NO_2 in Russia and Asia (MADRAS) during the period 2007–2012: instrumentation, elucidation of climatology, and comparisons with OMI satellite observations and global model simulations, Atmos. Chem. Phys., 14, 7909–7927, doi:10.5194/acp-14-7909-2014, 2014.

Kulbachevski: Report on the State of the Environment in Moscow in 2013, The Department for nature use and environment protection of Moscow Government, available at: http://www.mosecom.ru/reports/2013/report2013.pdf (last access: 17 July 2015), 224 pp., 2014 (in Russian).

Martin, R. V., Sioris, C. E., Chance, K., Ryerson, T. B., Wooldridge, P. J., Cohen, R. C., Neuman, J. A., Swanson, A., and Flocke, F. M.: Evaluation of space-based constraints on global nitrogen oxide emissions with regional aircraft measurements over and downwind if eastern North America, J. Geophys. Res., 111, D15308, doi:10.1029/2005JD006680, 2006.

AMTD
8, 7843–7878, 2015

Madronich, S., Flocke, S.: Handbook of Environmental Chemistry, edited by: Boule, P., Springer-Verlag, Heidelberg, 1–26, 1998.
O'Neill, N., Eck, T. F., Smirnov, A., Holben, B. N., and Thulasiraman, S.: Spectral discrimination of coarse and fine mode optical depth, J. Geophys. Res., 108, 4559–4573, doi:10.1029/2002JD002975, 2003.
O'Neill, N. T., Eck, T. F., Holben, B. N., Smirnov, A., and Dubovik, O.: Bimodal size distribution influences on the variation of Angstrom derivatives in spectral and optical depth space, J. Geophys. Res., 106, 9787–9806, doi:10.1029/2000JD900245, 2001.
Putaud, J. P., Cavalli, F., Martins dos Santos, S., and Dell'Acqua, A.: Long-term trends in aerosol optical characteristics in the Po Valley, Italy, Atmos. Chem. Phys., 14, 9129–9136, doi:10.5194/acp-14-9129-2014, 2014.
Richter, A., Burrows, J. P., Nüß, H., Granier, C., Niemeier, U.: Increase in tropospheric nitrogen dioxide over China observed from space, Nature, 437, 129–132, 2005.
Uliumdzhieva, N., Chubarova, N., and Smirnov, A.: Aerosol characteristics of the atmosphere over Moscow from Cimel sun photometer data, Meteorol. Hydrol., 1, 48–57, 2005.
Smirnov, A., Holben, B., Eck, T., Dubovik, O., and Slutsker, I.: Cloud screening and quality control algorithms for the AERONET data base, Remote Sens. Environ., 73, 337–349, 2000.
Tegen, I., Hollrig, P., Chin, M., Fung, I., Jacob, D., Penner, J.: Contribution of different aerosol species to the global aerosol extinction optical thickness: estimates from model results, J. Geophys. Res., 102, 23895–23915, doi:10.1029/97JD01864, 1997.
Yoon, J., Burrows, J. P., Vountas, M., von Hoyningen-Huene, W., Chang, D. Y., Richter, A., and Hilboll, A.: Changes in atmospheric aerosol loading retrieved from space-based measurements during the past decade, Atmos. Chem. Phys., 14, 6881–6902, doi:10.5194/acp-14-6881-2014, 2014.

AMTD
8, 7843–7878, 2015

Table 1. The monthly mean total NO_2 content according to the new climatology and NO_2 used in the standard AERONET algorithm; total NO_2 optical thickness at different wavelengths, and the difference in Angstrom exponent obtained with and without additional NO_2 correction of aerosol optical thickness at different wavelengths. Moscow, 2002–2013.

months	total* NO_2 content, DU*	NO_2 content used in the standard AERONET algorithm	total* NO_2 optical thickness at different wavelengths, nm				difference in Angstrom exponent	
			340	380	440	500	440–870 nm	340–380 nm
1	1.69	0.401	0.018	0.027	0.023	0.010	−0.22	0.55
2	1.96	0.607	0.022	0.032	0.027	0.012	−0.15	0.38
3	1.82	0.809	0.020	0.029	0.025	0.011	−0.10	0.24
4	1.60	0.429	0.017	0.026	0.022	0.010	−0.08	0.21
5	1.35	0.373	0.015	0.022	0.018	0.008	−0.08	0.21
6	1.13	0.278	0.012	0.018	0.015	0.007	−0.09	0.22
7	1.29	0.526	0.014	0.021	0.018	0.008	−0.05	0.13
8	1.34	0.474	0.015	0.022	0.018	0.008	−0.05	0.12
9	1.23	0.297	0.013	0.020	0.017	0.007	−0.07	0.16
10	1.24	0.371	0.014	0.020	0.017	0.007	−0.11	0.29
11	1.47	0.518	0.016	0.024	0.020	0.009	−0.18	0.44
12	1.62	0.285	0.018	0.026	0.022	0.010	−0.33	0.78
year	1.48	0.45	0.02	0.02	0.02	0.01	−0.13	0.31

* Total NO_2 content partly includes the NO_2 content which is applied in the standard AERONET correction algorithm.

AMTD
8, 7843–7878, 2015

Table 2. The main statistics of aerosol optical thickness at different wavelengths, water vapor content, and Angstrom exponent $\alpha_{440-870}$ in Moscow. The revised AERONET dataset. 2001–2014.

Months	1	2	3	4	5	6	7	8	9	10	11	12	year average
Day number	33	68	144	191	227	244	290	243	186	87	33	4	146
mean													
AOT340	0.12	0.23	0.25	0.36	0.32	0.25	0.38	0.46	0.38	0.22	0.17	0.12	0.27
AOT380	0.11	0.20	0.22	0.31	0.28	0.22	0.33	0.41	0.34	0.19	0.15	0.11	0.24
AOT440	0.09	0.17	0.19	0.26	0.23	0.18	0.27	0.35	0.29	0.16	0.13	0.09	0.20
AOT500	0.08	0.14	0.16	0.22	0.19	0.15	0.23	0.30	0.25	0.14	0.11	0.08	0.17
AOT675	0.05	0.09	0.10	0.14	0.12	0.09	0.14	0.19	0.16	0.09	0.07	0.06	0.11
AOT870	0.04	0.07	0.08	0.10	0.09	0.07	0.09	0.13	0.11	0.06	0.05	0.04	0.08
AOT1020	0.04	0.07	0.07	0.08	0.08	0.06	0.07	0.10	0.09	0.05	0.05	0.05	0.07
H20 content, cm	0.27	0.29	0.50	0.70	1.35	1.69	2.21	2.02	1.55	0.91	0.58	0.37	1.04
Angstrom exponent	1.24	1.30	1.27	1.39	1.35	1.50	1.63	1.55	1.47	1.35	1.30	1.30	1.39
standard deviation													
AOT340	0.09	0.15	0.19	0.26	0.19	0.15	0.29	0.50	0.42	0.15	0.12	0.04	0.21
AOT380	0.08	0.14	0.17	0.23	0.17	0.13	0.26	0.48	0.39	0.14	0.11	0.04	0.20
AOT440	0.07	0.12	0.14	0.19	0.14	0.11	0.23	0.45	0.34	0.12	0.09	0.04	0.17
AOT500	0.06	0.10	0.12	0.15	0.11	0.09	0.19	0.41	0.30	0.10	0.07	0.04	0.14
AOT675	0.04	0.07	0.08	0.09	0.07	0.05	0.12	0.29	0.19	0.06	0.05	0.04	0.09
AOT870	0.02	0.05	0.05	0.06	0.05	0.04	0.07	0.20	0.13	0.04	0.03	0.03	0.06
AOT1020	0.02	0.04	0.04	0.04	0.05	0.03	0.05	0.15	0.09	0.03	0.03	0.02	0.05
H20 content, cm	0.12	0.09	0.25	0.28	0.56	0.54	0.50	0.53	0.47	0.41	0.28	0.14	0.35
Angstrom exponent	0.24	0.28	0.29	0.23	0.29	0.25	0.17	0.18	0.21	0.24	0.16	0.35	0.24
confidence interval $P = 95\,\%$													
AOT340	0.03	0.04	0.03	0.04	0.02	0.02	0.03	0.06	0.06	0.03	0.04	0.04	0.04
AOT380	0.03	0.03	0.03	0.03	0.02	0.02	0.03	0.06	0.06	0.03	0.04	0.04	0.03
AOT440	0.02	0.03	0.02	0.03	0.02	0.01	0.03	0.06	0.05	0.02	0.03	0.04	0.03
AOT500	0.02	0.02	0.02	0.02	0.01	0.01	0.02	0.05	0.04	0.02	0.02	0.04	0.03
AOT675	0.01	0.02	0.01	0.01	0.01	0.01	0.01	0.04	0.03	0.01	0.02	0.04	0.02
AOT870	0.01	0.01	0.01	0.01	0.01	0.00	0.01	0.02	0.02	0.01	0.01	0.03	0.01
AOT1020	0.01	0.01	0.01	0.01	0.01	0.00	0.01	0.02	0.01	0.01	0.01	0.02	0.01
H20 content, cm	0.04	0.02	0.04	0.04	0.07	0.07	0.06	0.07	0.07	0.09	0.10	0.14	0.07
Angstrom exponent,	0.08	0.07	0.05	0.03	0.04	0.03	0.02	0.02	0.03	0.05	0.05	0.34	0.07

AMTD
8, 7843–7878, 2015

Table 2. Continued.

Months	1	2	3	4	5	6	7	8	9	10	11	12	year average
Day number	33	68	144	191	227	244	290	243	186	87	33	4	146
50 %quantile													
AOT340	0.11	0.18	0.23	0.37	0.32	0.24	0.35	0.32	0.28	0.18	0.16	0.12	0.24
AOT380	0.10	0.15	0.21	0.32	0.27	0.21	0.30	0.29	0.25	0.15	0.14	0.10	0.21
AOT440	0.08	0.13	0.17	0.26	0.22	0.17	0.25	0.24	0.21	0.13	0.12	0.08	0.17
AOT500	0.07	0.11	0.14	0.22	0.19	0.15	0.21	0.20	0.18	0.12	0.11	0.07	0.15
AOT675	0.05	0.08	0.09	0.14	0.12	0.09	0.13	0.13	0.11	0.07	0.07	0.04	0.09
AOT870	0.04	0.06	0.07	0.10	0.09	0.07	0.09	0.08	0.08	0.05	0.05	0.03	0.07
AOT1020	0.04	0.06	0.06	0.08	0.07	0.06	0.07	0.07	0.06	0.04	0.05	0.04	0.06
H20 content, cm	0.28	0.29	0.48	0.70	1.45	1.69	2.17	2.11	1.57	0.87	0.52	0.41	1.04
Angstrom exponent	1.46	1.40	1.42	1.49	1.41	1.59	1.69	1.61	1.54	1.47	1.39	1.72	1.52
maximum													
AOT340	0.37	0.62	1.10	1.52	1.37	0.87	3.19	3.79	2.90	0.77	0.70	0.20	1.45
AOT380	0.34	0.58	0.95	1.34	1.20	0.76	2.97	3.78	2.74	0.70	0.60	0.17	1.35
AOT440	0.30	0.51	0.79	1.10	0.96	0.66	2.60	3.63	2.46	0.57	0.48	0.16	1.18
AOT500	0.27	0.45	0.65	0.89	0.77	0.57	2.25	3.46	2.16	0.45	0.39	0.15	1.04
AOT675	0.18	0.32	0.42	0.51	0.42	0.36	1.42	2.66	1.41	0.27	0.26	0.12	0.70
AOT870	0.13	0.24	0.32	0.31	0.29	0.24	0.89	1.85	0.89	0.18	0.19	0.09	0.47
AOT1020	0.10	0.20	0.28	0.24	0.28	0.22	0.64	1.41	0.65	0.15	0.17	0.08	0.37
H20 content, cm	0.60	0.52	1.39	1.80	3.11	3.16	3.46	3.53	2.82	2.11	1.29	0.55	2.03
Angstrom exponent	1.86	1.89	1.86	1.93	1.98	2.12	2.11	1.94	1.96	1.88	1.72	1.82	1.92
minimum													
AOT340	0.03	0.05	0.06	0.04	0.08	0.05	0.10	0.08	0.07	0.07	0.05	0.11	0.07
AOT380	0.03	0.04	0.03	0.03	0.06	0.03	0.05	0.04	0.04	0.04	0.02	0.07	0.04
AOT440	0.02	0.03	0.03	0.03	0.05	0.03	0.05	0.04	0.03	0.03	0.02	0.05	0.04
AOT500	0.02	0.02	0.03	0.03	0.04	0.03	0.05	0.04	0.03	0.03	0.02	0.05	0.03
AOT675	0.01	0.02	0.02	0.02	0.03	0.02	0.03	0.02	0.02	0.02	0.02	0.03	0.02
AOT870	0.01	0.02	0.02	0.02	0.03	0.02	0.02	0.02	0.02	0.02	0.01	0.02	0.02
AOT1020	0.02	0.03	0.02	0.02	0.02	0.01	0.01	0.01	0.01	0.02	0.02	0.02	0.02
H20 content, cm	0.07	0.11	0.16	0.20	0.50	0.64	1.12	0.90	0.53	0.24	0.21	0.16	0.40
Angstrom exponent	0.96	0.72	0.56	0.82	0.42	0.43	1.04	1.02	0.44	0.86	1.01	0.96	0.77

AMTD
8, 7843–7878, 2015

Table 3. Correlation coefficients and AOT500 trends (% yr^{-1}) over 2001–2014 in monthly mean, 50 % quantile and daily maxima. Statistically significant values at P = 95 % are shown in bold. Moscow.

months	average		50 % quantile		daily maxima	
	correlation coefficient	trend,% yr^{-1}	correlation coefficient	trend,% yr^{-1}	correlation coefficient	trend,% yr^{-1}
2	−0.14	−2 %	−0.08	−1 %	−0.28	−4 %
3	−0.30	−3 %	−0.36	−4 %	−0.09	−1 %
4	**−0.67**	**−5 %**	**−0.64**	**−7 %**	**−0.48**	**−4 %**
5	**−0.52**	**−2 %**	0.19	1 %	**−0.69**	**−6 %**
6	−0.04	0 %	0.00	0 %	0.02	0 %
7 *	−0.38/−0.51	−3 %/−1 %	−0.10/−0.14	−1 %/−1 %	−0.46/−0.18	−10 %/−1 %
8 *	0.01/−0.47	0 %/−1 %	0.03/−0.19	1 %/−1 %	0.04/−0.14	1 %/−1 %
9 *	**−0.50**/**−0.50**	**−10–3 %**	**−0.48**/ − 0.43	**−10 %**/−3 %	**−0.58**/**−0.72**	**−14 %**/**−7 %**
10	−0.05	−1 %	−0.08	−1 %	−0.04	−1 %
11	0.09	1 %	0.09	1 %	0.05	1 %

* First value corresponds to the whole statistics and the second one – to the statistics without forest fires episodes observed in 2002 and 2010.

AMTD
8, 7843–7878, 2015

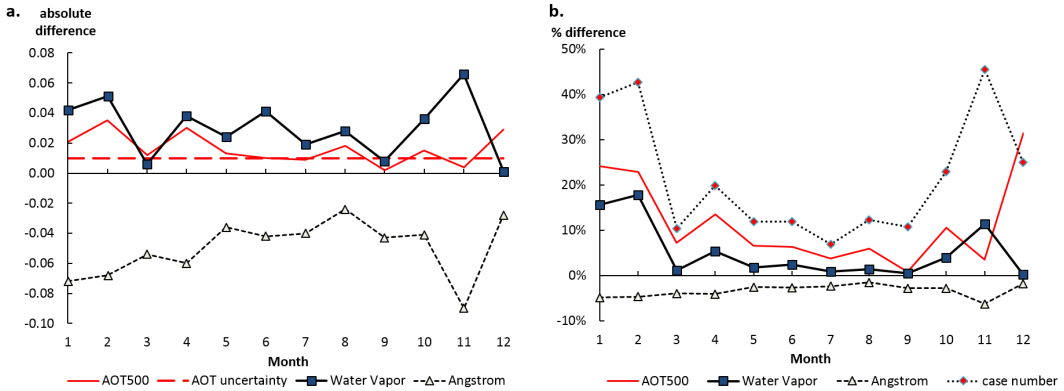

Figure 1. The absolute **(a)** and relative **(b)** difference of monthly mean standard level 2.0 data on aerosol optical thickness at 500 nm (AOT500), Angstrom exponent and water vapor with the dataset after additional cloud correction. The standard uncertainty of AOT measurements is shown in Fig. 1a. Relative changes in day number removed after additional cloud correction is shown in Fig. 1b. Moscow, 2001–2014 period.

AMTD
8, 7843–7878, 2015

Long-term variability of aerosol optical thickness in Eastern Europe over 2001–2014

N. Y. Chubarova et al.

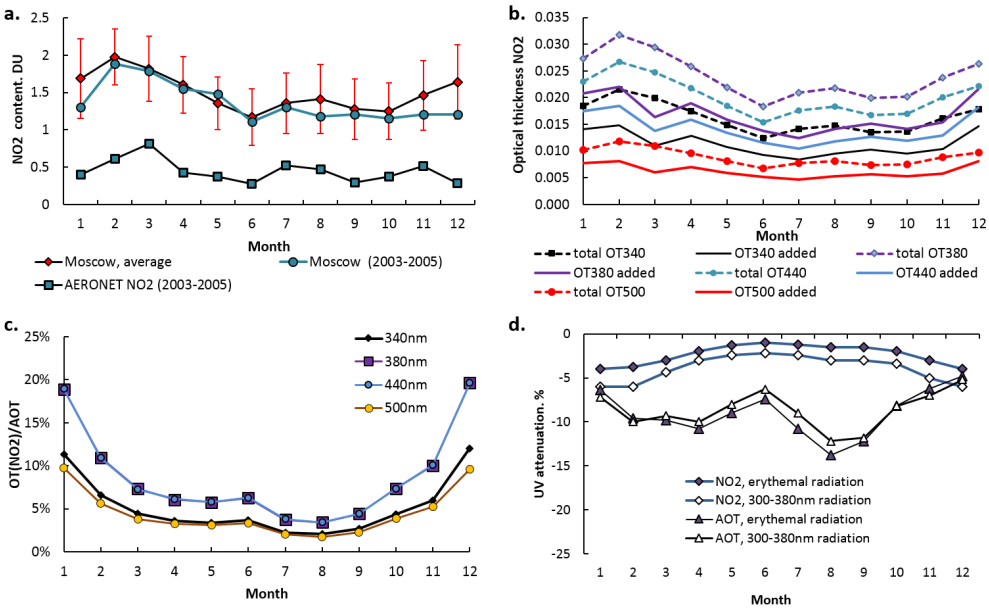

Figure 2. The seasonal distribution of mean NO_2 content over 2002–2013 and 2003–2005 periods obtained according to (Chubarova et al., 2009) and the NO_2 retrievals applied in the standard AERONET algorithm **(a)**; monthly mean total and additional optical thickness (OT) of NO_2 at different wavelengths **(b)**; monthly mean ratio OT(NO_2)/AOT at different wavelengths **(c)**; relative attenuation of erythemal radiation and UV radiation 300–380 nm due to NO_2 and AOT at noon time conditions according to the results of 8-stream DISORT method **(d)**. Moscow.

AMTD
8, 7843–7878, 2015

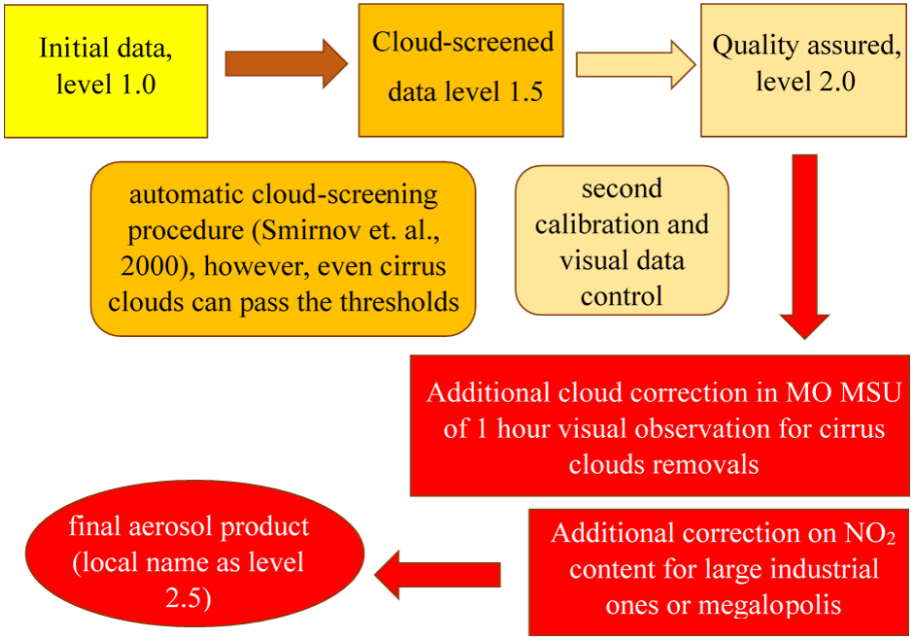

Figure 3. The scheme of the updated AERONET data proceeding with additional cloud and NO_2 correction used at the Moscow MSU MO.

AMTD
8, 7843–7878, 2015

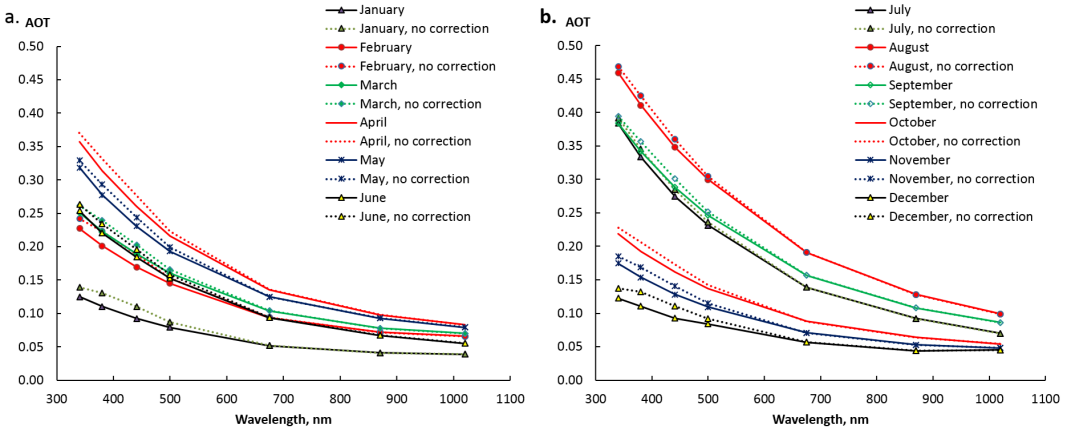

Figure 4. Spectral dependence of monthly mean AOT according to standard and the revised AERONET dataset with the additional cloud and NO_2 correction. Moscow, 2001–2014 period.

AMTD
8, 7843–7878, 2015

Long-term variability of aerosol optical thickness in Eastern Europe over 2001–2014

N. Y. Chubarova et al.

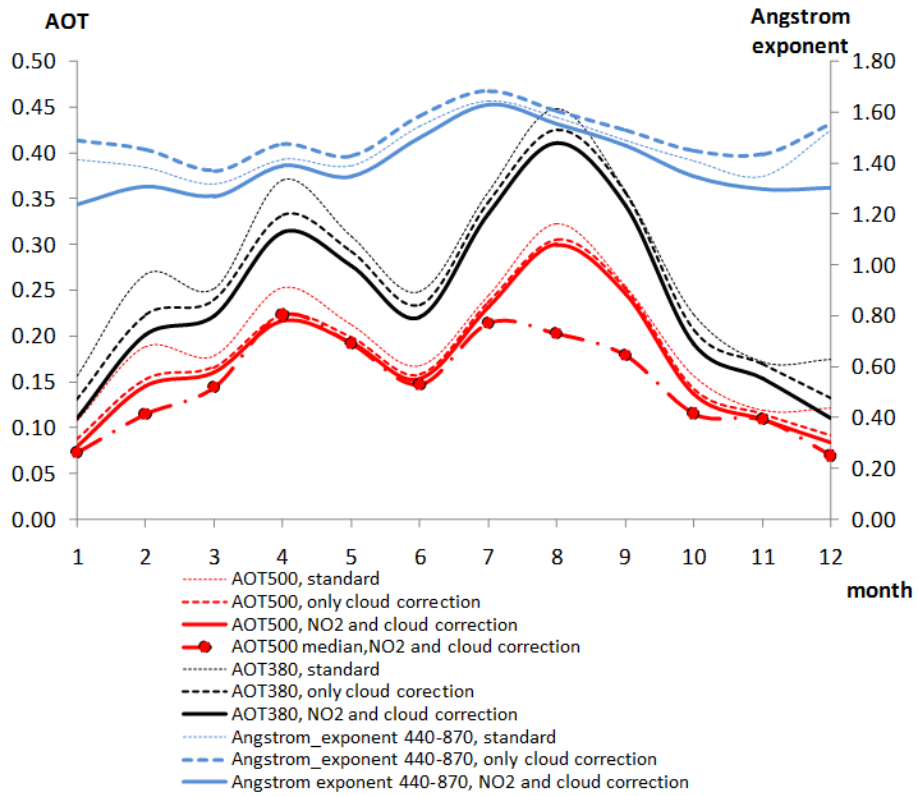

Figure 5. Seasonal variation of monthly mean aerosol optical thickness at 380 and 500 nm, median AOT at 500 nm, and Angstrom exponent according to the standard AERONET level 2.0 dataset, the data after additional cloud correction, and the final revised dataset. Note, that the additional correction of cloud and NO_2 has different sign for Angstrom exponent. Moscow, 2001–2014 period.

AMTD
8, 7843–7878, 2015

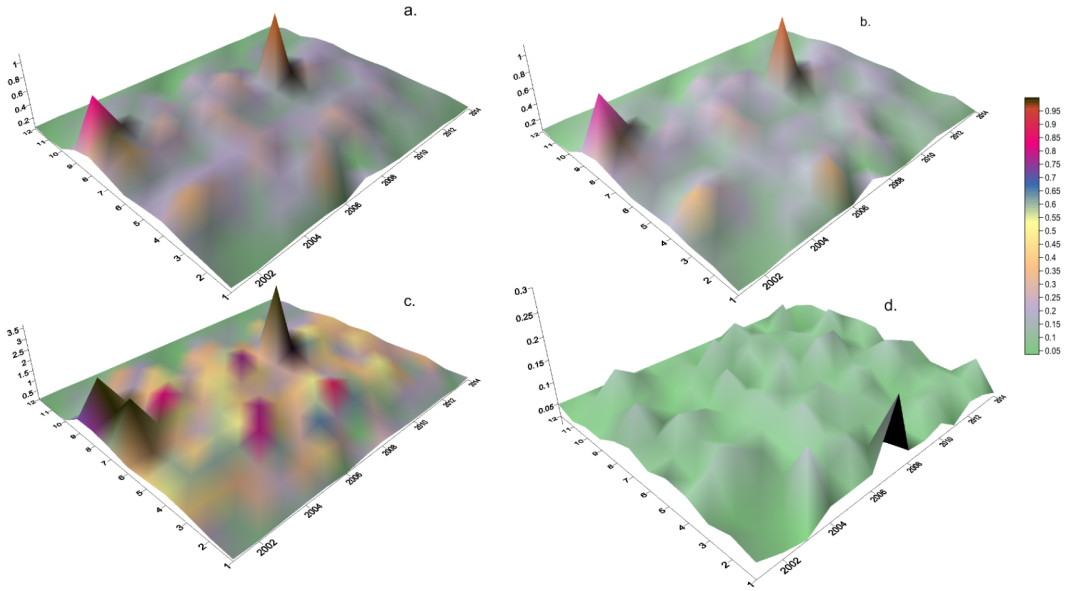

Figure 6. 3-D distribution of the revised monthly mean AOT500 **(a)**, 50 % quantile AOT500 **(b)**, daily AOT500 maximum **(c)** and daily AOT500 minimum **(d)**. Moscow.

AMTD
8, 7843–7878, 2015

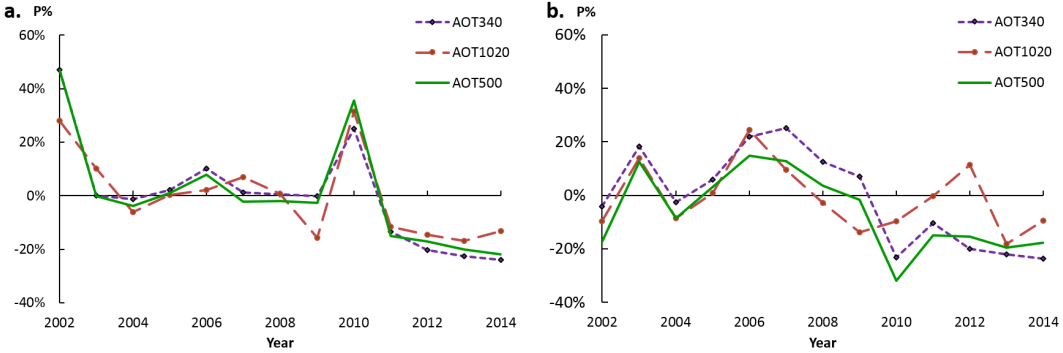

Figure 7. Interannual variations of the revised annual mean **(a)** and 50 % quantile **(b)** AOT at several wavelengths. Moscow. Comment: the annual 50 % quantile AOT is estimated from monthly 50 % quantile AOT values. For consistency the 2001 data were not used since the measurements have been in operation only since August.

AMTD
8, 7843–7878, 2015

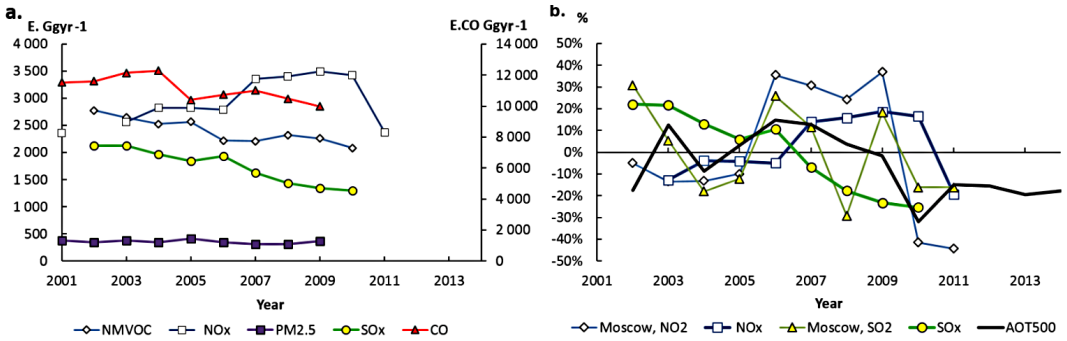

Figure 8. Interannual variations in emissions of main aerosol precursors and particulate matter ($PM_{2.5}$) according to WebDab - EMEP database **(a)** over European part of Russia **(a)**, relative changes in 50 % quantile AOT500 and in SO_2 and NO_x, emissions over European part of Russia and directly over Moscow **(b)**.

AMTD
8, 7843–7878, 2015